Mem. S.A.It. Vol. 77, 927
© SAIt 2006
Memorie della

Nuclear uncertainties on pre-explosive ^{26}Al nucleosynthesis.

C. Baldovin, M. Pignatari, and R. Gallino

Dipartimento di Fisica Generale dell'Università di Torino, Via P. Giuria 1, 10125 Torino, Italy e-mail: baldovin@studenti.ph.unito.it

Abstract. We present a study on the radioactive isotope ^{26}Al nucleosynthesis in massive stars in the post main sequence evolutionary stage of convective shell carbon burning, following a model of a 25 $M_\odot$ and solar metallicity.

Key words. massive stars – nucleosynthesis

1. Introduction

Evidence of the radioactive isotope ^{26}Al ($t_{1/2}$ = 7.2×10^5 yr) in the Galaxy has been found through its positron emission (β^+) product ^{26}Mg*, which de−excites emitting a gamma ray line at 1.809 MeV. The detected flux corresponds to an ^{26}Al equilibrium mass of 2.8±0.8 $M_\odot$ present in the Galaxy, inferred by INTEGRAL (Diehl et al. 2006). The spatial distribution is concentrated along the Galactic plane and is not uniform, but presents regions of prominent emission (Diehl et al. 1995) consistent with a massive star origin. Theoretical studies have predicted ^{26}Al nucleosynthesis in different astrophysical sources: Wolf Rayet stars (Palacios et al. 2005), AGB stars (Wasserburg et al. 1994), massive stars during pre−supernova stages (Arnett & Wefel 1978; Chieffi & Limongi 2006) and during core collapse supernova by explosive nucleosynthesis (Woosley & Weaver 1995; Timmes et al. 1995; Chieffi & Limongi 2003, 2005).

Send offprint requests to: C. Baldovin

We focus our study of the ^{26}Al nucleosynthesis on a 25 $M_\odot$ star with solar metallicity, during the convective shell carbon burning stage.

2. Convective shell C−burning and ^{26}Al nucleosynthesis: Overview

In advanced stellar evolution of massive stars, carbon burns in the center of the star and then in outer convective shell(s). For a 25 $M_\odot$ star, typically two convective carbon burning shells form. For example in Chieffi et al. (1998) the second shell involves approximately 2.3 $M_\odot$, from 2.3 to 4.6 $M_\odot$. At the convective carbon shell bottom, density is $\rho \sim 10^5$ g/cm^3 and temperature is $T_9 \sim 1.1$ (T_9 is the temperature in units of 10^9 K) for the major part of carbon shell burning. Only in the last days before the explosive event, when ^{12}C abundance is sufficiently decreased, a thermal instability rapidly sets in raising the temperature in the C−shell to $T_9 \sim 1.3 - 1.4$ (Arnett & Wefel 1978; Chieffi & Limongi 2006).

^{12}C burns mainly through ^{12}C(^{12}C, α)^{23}Na and ^{12}C(^{12}C, p)^{20}Ne reactions (rate reference:

Caughlan & Fowler 1988). The most abundant isotopes at the end of carbon burning are: ^{16}O produced during previous helium burning and the carbon burning products ^{20}Ne and ^{23}Na. During convective shell carbon burning, ^{26}Al is produced by ^{25}Mg(p, γ)^{26}Al reaction. In 1978, Arnett and Wefel published their work on ^{26}Al production in a massive star during carbon burning in a convective shell at temperature $T_9 \sim 1.1 - 1.3$. Reaction rates used were: ^{25}Mg(p, γ)^{26}Al from Wagoner (1969) and ^{26}Al β^+ decay rate from Hansen (1966, unpublished data). In their model, approximately 50% of the carbon is consumed by shell C−burning. Of this carbon, resulting at the end of convective core He burning, the first 75% burns at the relatively constant temperature $T_9 \sim 1.1$, then the temperature raises to $T_9 \sim 1.3 - 1.4$ just before the supernova explosion. Fig. 1 reports the results by Arnett and Wefel (1978). In the upper panel the ^{26}Al and ^{27}Al mass fractions are plotted as a function of the ^{12}C mole fraction during carbon shell depletion in the convective shell, the lower panel shows the density and temperature profiles. At the beginning of carbon burning, ^{26}Al is produced, then its abundance remains roughly constant as long as the carbon shell temperature remains unchanged ($T_9 \sim 1.1$). After the ^{12}C is depleted from the initial Y(^{12}C)=2.6×10^{-2} to Y(^{12}C)=1.6×10^{-2}, the temperature raises. Despite the reduction in the ^{12}C fuel, because of the strong carbon burning rate dependence on temperature there is an important production of protons via ^{12}C(^{12}C, p)^{20}Ne. Consequently, ^{26}Al is strongly produced. The ^{27}Al mass fraction, produced by ^{26}Mg(p, γ)^{27}Al, monotonically increases during all the carbon burning phase. The final isotopic ratio obtained from this work was ^{26}Al/^{27}Al = 1.7×10^{-3}.

On the other hand, Woosley & Weaver (1980) concluded that ^{26}Al in a massive star is mostly produced during explosive neon burning. They confirmed that ^{26}Al is also produced during the last phase of convective shell carbon burning when the temperature is raised, but pointed out that the final distribution of ^{26}Al in the C-shell depends on how efficiently convection works. In Woosley & Weaver (1980)

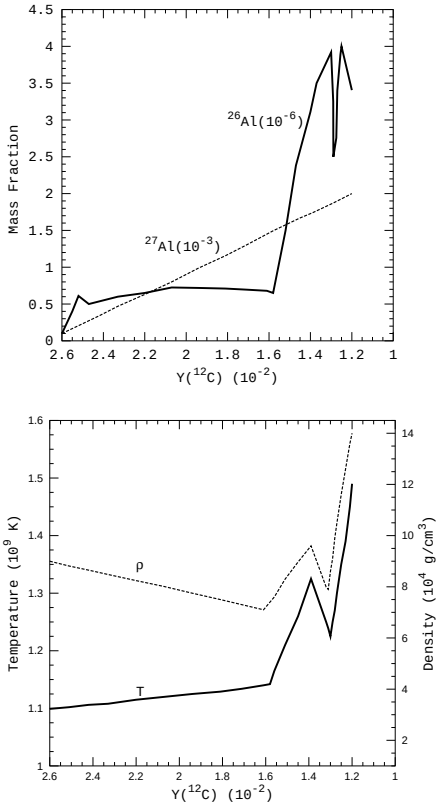

Fig. 1. Evolution of the carbon shell from Arnett & Wefel (1978) calculations. In the lower panel, density and temperature are plotted as a function of the mole fraction of ^{12}C, Y(^{12}C). Upper panel shows evolution of ^{26}Al and ^{27}Al mass fraction.

the final ratio ^{26}Al/^{27}Al was $\sim 10^{-3}$. This work used ^{26}Al β^+ decay rate published by Ward & Fowler (1980), where it was shown that ^{26}Al^0 and ^{26}Al^m become fully thermalized for temperatures $T_9 > 0.4$ (see §3).

Woosley & Weaver (1995) followed the evolution and the explosion for a wide range of massive stars (11 - 40 M$_\odot$). Timmes et al. (1995) analysed the ^{26}Al production using the 25 M$_\odot$ model by Woosley & Weaver (1995). Fig. 2 reports their results, where is shown that a large fraction of ^{26}Al is produced by explosive nucleosynthesis. They pointed out that ν interactions enhance the final ^{26}Al yields, liberating protons for the occurrence of the ^{25}Mg(p, γ)^{26}Al reaction.

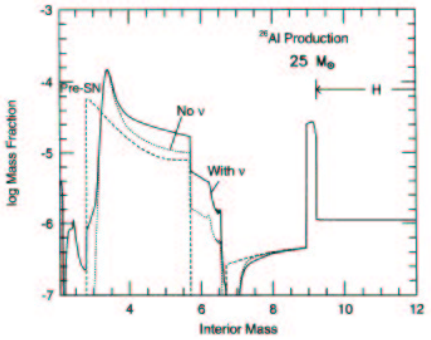

Fig. 2. ^{26}Al mass fraction against mass coordinate for a solar metallicity, 25 M$_\odot$ star from Timmes et al. (1995). Pre-supernova production in dashed line and the explosive contribution with (solid line) and without (dotted line) ν-process enhancement are shown.

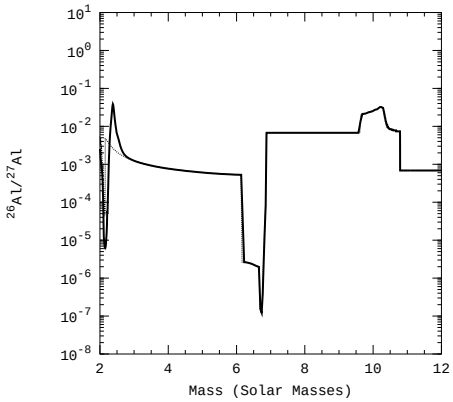

Fig. 3. ^{26}Al/^{27}Al against mass coordinate is plotted from Chieffi & Limongi (2006), 25 M$_\odot$ model. Dotted and solid lines represent pre−supernova and explosive contribution, respectively. Pre−supernova convective C−shell is comprised between 2.2 M$_\odot$ and 6.25 M$_\odot$.(Data from Limongi M. webpage)

Fig. 3 shows the results of a model of 25 M$_\odot$ star of solar metallicity by Chieffi & Limongi (2006). The convective carbon burning zone is comprised between 2.2 M$_\odot$ and 6.25 M$_\odot$. With respect to the pre−supernova phase, the main part of the convective shell shows unchanged ^{26}Al/^{27}Al after the explosion, but at the bottom of the shell the pre−explosive ^{26}Al is destroyed and strongly rebuilt by explosive nucleosynthesis. About 70% of the total ^{26}Al ejected is produced explosively, while the remaining has been synthesised during the previous convective shell carbon burning phase. A minor fraction results from core H− burning, partially mixed over the whole envelope during the first dredge up.

3. ^{26}Al Properties

The ^{26}Al ground state (^{26}Al^0) has a half-life of $t_{1/2} = 7.2 \times 10^5$ yr, while for the isomer (^{26}Al^m) the half-life is $t_{1/2} = 6.35$ s. Both states are consistently feed by the ^{25}Mg(p, γ)^{26}Al reaction. Particular attention must be payed to whether treating ^{26}Al as a thermal mixture between the ground state and its isomer, or as two physically distinct nuclei. According to Ward & Fowler (1980), for $T_9 < 0.4$ the equilibration time between the isomer and the ground state is longer than the time scale for nuclear reactions ($\tau_{eq} \geq \tau_{nuc}$). This implies that, for $T_9 < 0.4$, ^{26}Al^0 and ^{26}Al^m are not thermalized, and must be treated as two separated nuclei. At shell carbon burning temperatures instead, the two states are fully thermalized. Table 1 reports the ^{26}Al β^+ decay rates from two different calculations; Fuller et al. 1985 (FFN85) and Runkle et al. 2001. The difference between both calculations lays within $\sim 20\%$.
Assuming steady production of ^{26}Al (Arnett & Wefel 1978) one has:

$$\frac{Y(^{26}Al)}{Y(^{25}Mg)} = \frac{Y(p)\rho N_A < \sigma v >_{p,\gamma}}{(\lambda_{26} + Y(n)\rho N_A < \sigma v >_{n,p})} \quad (1)$$

Table 1. Comparison between ^{26}Al β^+ decay rates from Fuller et al. (1985) and Runkle et al. (2001) in the temperature range $1.0 \leq T_9 \leq 1.5$. They are consistent within 20%.

T_9	$\lambda_{26}(s^{-1})$	
	FFN85	Runkle 2001
1.0	$8.45E-4$	$7.00E-4$
1.1	$1.03E-3$	$8.88E-4$
1.2	$1.23E-3$	$1.08E-3$
1.3	$1.45E-3$	$1.28E-3$
1.4	$1.72E-3$	$1.47E-3$
1.5	$1.99E-3$	$1.66E-3$

Table 2. References of the rates involved in ^{26}Al nucleosynthesis for $T_9 = 1.1$: NACRE= Angulo et al. 1999, NETGEN5.0= Jorissen & Goriely 2001, Bao2000= Bao et al. 2000, RT 2000= Rauscher & Thielemann 2000, KO97= Koehler et al. 1997

Reaction	$N_A < \sigma v >$(cm^{3}mole^{-1}s^{-1})	Source
^{25}Mg(p, γ)^{26}Al	1.1×10^3	NACRE
^{26}Al(p, γ)^{27}Si	3.4×10^2	NACRE
^{26}Al(α, p)^{29}Si	3.8×10^{-4}	NETGEN5.0
^{26}Al(n, γ)^{27}Al	4.6×10^5	Bao2000
^{26}Al(n, α)^{23}Na	1.6×10^7	RT 2000
^{26}Al(n, p)^{26}Mg	3.2×10^7	KO97

The numerator on the right side of equation (1) is the term of ^{26}Al production by proton capture on ^{25}Mg while the denominator represents the two main destruction reactions of ^{26}Al: ^{26}Al(β^+)^{26}Mg and ^{26}Al(n, p)^{26}Mg (see Table 2) ρ is the shell density, Y(i) = $X_i/A_i = n_i/\rho N_A$ is the molar fraction of the i species and $N_A < \sigma v >$ the reaction rate in units of cm^{3}mole^{-1}s^{-1} with N_A Avogadro's number. Neutrons are provided by the reaction ^{22}Ne(α, n)^{25}Mg on the residual ^{22}Ne left after core He exhaustion. Taking into account the characteristic carbon burning shell bottom density ($\rho \sim 10^5$ g/cm^3) and the reaction rates involved, it is possible to conclude that at least during the first phase at constant temperature, the dominant depletion channel is the ^{26}Al decay into ^{26}Mg. For example, if we consider carbon burning at the temperature $T_9 = 1.1$, the condition for the ^{26}Al(n, p)^{26}Mg channel to be comparable with ^{26}Al(β^+)^{26}Mg decay is that $N_n \geq 10^{12}$cm^{-3}. From our calculations (see §4), the maximum neutron density reached at this temperature is a factor of 5−10 lower with respect the above requested neutron density. In this phase, the rising amount of neutrons depends on the more efficient α−particles production by ^{12}C(^{12}C, α)^{23}Na reactions and on how much ^{22}Ne is still available to provide neutrons.

In explosive conditions, ^{26}Al is produced by ^{25}Mg(p, γ)^{26}Al and ν interactions, the most important depletion channel is ^{26}Al(n, p)^{26}Mg. Obviously, ^{26}Al(β^+)^{26}Mg is not important anymore owing the short explosive time scale.

4. Calculations

The convective core He burning phase was followed according to the physical inputs from the FRANEC evolutionary code (Chieffi & Straniero 1989). The nucleosynthesis of the subsequent carbon burning phase was then calculated using a post processing model (see Raiteri et al. 1991) with an updated network extended to all unstable isotopes as far as the β−decay is longer than 5 min. Neutron captures, α−captures, proton−captures, β^+ and β^- decays and important photodisintegrations, as ^{13}N(γ, p)^{12}C, ^{21}Na(γ, p)^{20}Na and ^{17}O(γ, n)^{16}O are included.

Our calculations consider a one zone model that evolves in two phases, each of them at constant temperature. The first phase lasts until the ^{12}C mass fraction drops from the initial X(^{12}C) = 0.178 to 0.103. After that, starts the second phase at higher temperature. The evolution follows until X(^{12}C) = 5.0×10^{-2}. Two different initial temperatures were considered for the first phase: $T_9 = 1.05$ and 1.1. In both cases, the second part of the carbon burning was set at $T_9 = 1.3$. References of the main rates involved on the ^{26}Al are listed on Table 2. For the ^{26}Al β^+ decay rate we used the rate of Fuller et al. (1985).

Fig. 4 shows the ^{26}Al and ^{27}Al trend during carbon burning in a $T_9 = 1.05$ shell. The ^{26}Al, ^{27}Al mass fractions and their isotopic ratio are plotted as a function of the ^{12}C mass fraction. Scale for the isotopic ratio is on the left side and for the mass fraction on the right side. We observe that as long as carbon is depleted

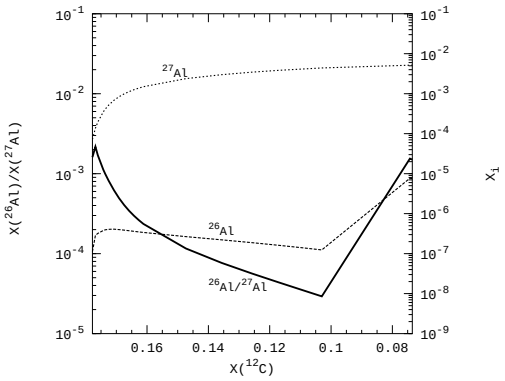

Fig. 4. M=25 M$_\odot$, [Fe/H]=0, T_9 = 1.05 − 1.3. Solid line represents the ^{26}Al/^{27}Al ratio, thick dotted and thin dotted lines represent the ^{26}Al and ^{27}Al mass fractions, respectively. Scale for the isotopic ratio on the left side and for the mass fractions on the right side.

during the first part of burning, ^{26}Al/^{27}Al decreases from 2.2×10^{-3} down to 2.9×10^{-5}. ^{26}Al is produced in the first day of carbon ignition, because of the high protons abundance deriving from the ^{12}C(^{12}C, p)^{20}Ne reaction. Subsequently, ^{26}Al is depleted by the beta decay channel according to §3, while ^{27}Al increases monotonically. In the second part of the burning (Δt ∼ 0.5 days), with the shell at higher temperature (T_9 = 1.3), ^{26}Al increases and consequently ^{26}Al/^{27}Al raises up to 1.5×10^{-3}.

Taking into account the nuclear reaction rates involved in the ^{26}Al production and depletion, we tested how the isotopic ratio ^{26}Al/^{27}Al is affected by variations in these rates.

In Fig. 5 the results obtained on some tests made for the case $T_9 = 1.1 - 1.3$ are shown. At T_9 = 1.1, in the standard case (solid line), after carbon ignition the ratio ^{26}Al/^{27}Al gets to a higher value 4.2×10^{-3} than in the precedent lower temperature case (T_9 = 1.05), then decreases down to 7.0×10^{-5} (and raises again to 8.6×10^{-4} when the shell is turned to the higher temperature). The thin dotted line on Fig. 5 represents the ^{26}Al/^{27}Al ratio when ^{25}Mg(p, γ)^{26}Al is increased by a factor 2. In this case the ratio gets to 8.2×10^{-3} at the beginning of carbon burning and to 1.4×10^{-3} when the shell temperature is raised, which represents a 60% higher value than in the standard case. When λ_{26} is diminished by a factor of 2 (thick dotted line on Fig. 5) at the beginning of the burning the ratio is 1.2×10^{-2}, and when the high temperature phase is active increases to 1.6×10^{-3}. This final value is 90% higher than the standard case.

As discussed in §3, the λ_{26} uncertainty is ∼ 20%. The test on λ_{26} takes into account the fact that ^{26}Al is produced in the shell bottom and it is fastly mixed into the upper layers at lower temperatures, where the decay times are longer.

The temperature behaviour in the shell, the convection velocity and the mass involved in the convection influence the effective ^{26}Al beta decay. In Fig. 5 we also report the ^{26}Al/^{27}Al ratio obtained using ^{26}Al terrestrial decay rate. In this case, as expected, the reaction ^{26}Al(n,p)^{26}Mg controls the ^{26}Al depletion during the whole C−shell evolution, instead of λ_{26}.

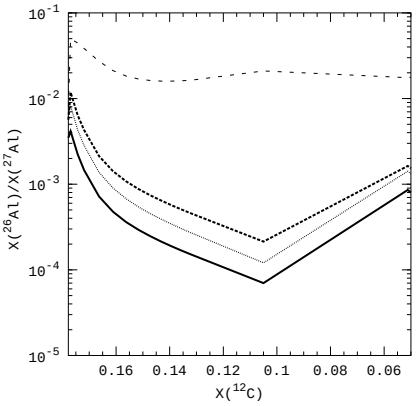

Fig. 5. M=25 M$_\odot$, [Fe/H]=0, T_9 = 1.1 − 1.3. Several ^{26}Al/^{27}Al ratios are plotted: the solid line represents the standard case, thin dotted line is the test with ^{25}Mg(p, γ) × 2, thick dotted line is the test with λ_{26}/2, dashed line is the test using the λ_{26} terrestrial value.

5. Conclusions

For the 25 $M_{\odot}$ model with solar metallicity, a not negligible ^{26}Al production from pre−supernova convective shell carbon burning is ejected in the final yields. The final rising temperature at the bottom of the convective carbon shell apports a fundamental contribution to the ^{26}Al abundance because of an efficient proton production from the $^{12}C(^{12}C, p)^{23}Na$ reaction.

In the first phase of carbon shell burning, ^{26}Al depletion is dominated by $^{26}Al(\beta^{+})^{26}Mg$. Only during the last phase, when the temperature raises, $^{26}Al(n, p)^{26}Mg$ starts to gain strength. Finally, we showed that the ^{26}Al nucleosynthesis is uncertain in convective shell C−burning by a factor of two.

Acknowledgements. We would like to thank Marco Limongi for helpful discussions.

References

Angulo, C., Arnould, M., Rayet, M. et al. 1999 Nucl. Phys. A, 656, 3
Arnett, D., Wefel, J.P 1978, ApJ, 224, L1359
Busso, M., Gallino, R., Wasserburg, G.J 2003 PASA, 20, 356
Caughlan, G.R. & Fowler, W.A. 1988 ADNDT, 40, 283
Chieffi, A. & Straniero, O. 1989 ApJS, 71, 47
Chieffi, A., Limongi, M., Straniero, O. 1998 ApJ, 502, 737
Chieffi, A. & Limongi, M. 2003 PASA, 20, 324
Chieffi, A. & Limongi, M. 2005 Nucl. Phys. A, 758, 11
Chieffi, A. & Limongi, M. 2006, Limongi M. homepage, http://www.mporzio.astro.it/~limongi
Diehl, R., Dupraz, C., Bennett, K., Bloemen, H. et al. 1995 A&A, 298, 445
Diehl, R., Halloin, H., Kretschmer, K. et al. 2006 Nature, 439, 45
Fuller, G.M., Fowler, W.A., Newman, M.J. 1985 ApJ, 239, 1
Jorissen, A., Goriely, S. 2001 Nucl. Phys. A, 688, 508
Koehler, P.E., Kavanagh, R.W. Vogelaar, R.D., Gledenov, Yu.M., Popov, Yu.P. 1997, PRC, 56 1138
Palacios, A., Meynet, G., Vuissouz, C. et al. 2005 A&A, 429, 613
Prantzos, N. 2004 A&A, 420, 1033
Raiteri, C.M., Busso, M., Gallino, R., Picchio, G. 1991 ApJ, 371, 665
Rauscher, T. & Thielemann, F. 2000 ADNDT, 75, Issue 1-2, 1
Runkle, R.C., Champange, A.E., Engel, J. 2001 ApJ, 556, 970
Timmes, F.X., Woosley, S.E., Hartman, D.H., et al. 1995 ApJ, 449, 204
Truran, J.W., Cameron, A.G.W. 1978 ApJ, 219, 226
Wagoner, R.V. 1969 ApJS, 18, 247
Ward, R., Fowler, W. 1980 ApJ, 238, 266
Wasserburg, G.J., Busso, M., Gallino, R., Raiteri, C.M. 1994 ApJ, 424, 412
Woosley, S.E., Weaver, T.A. 1980 ApJ, 238, 1017
Woosley, S.E., Weaver, T.A. 1995 ApJS, 101, 181